

Magnetosphere Terrestre:

un aperçu de la dynamique magnétosphérique



Laboratoire de Physique des Plasmas

Dominique Fontaine

Laboratoire de Physique des Plasmas

Ecole Polytechnique, France

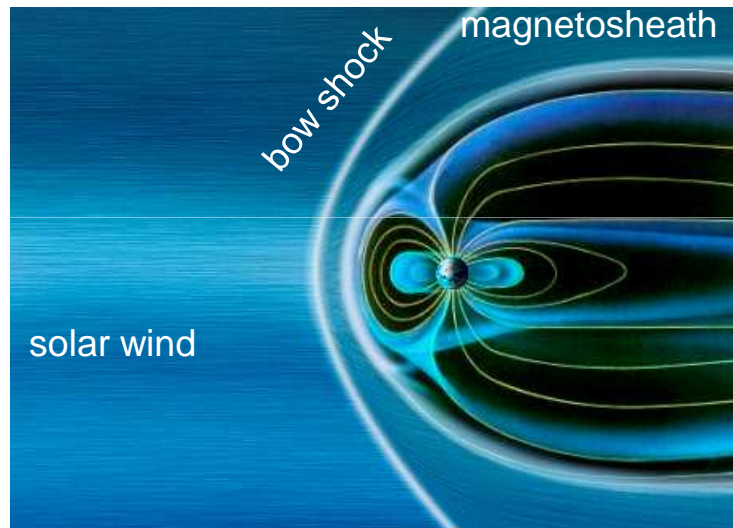


Outline

1. Solar wind drivers of the magnetospheric activity and coupling functions
2. Dynamics of the coupled magnetosphere – ionosphere system
3. Particle sources and outflows in the magnetosphere

1. Solar wind drivers of the magnetospheric dynamics

Formally, the magnetosphere is created by interaction of a magnetized body with the super-sonic super-Alfvénic solar wind

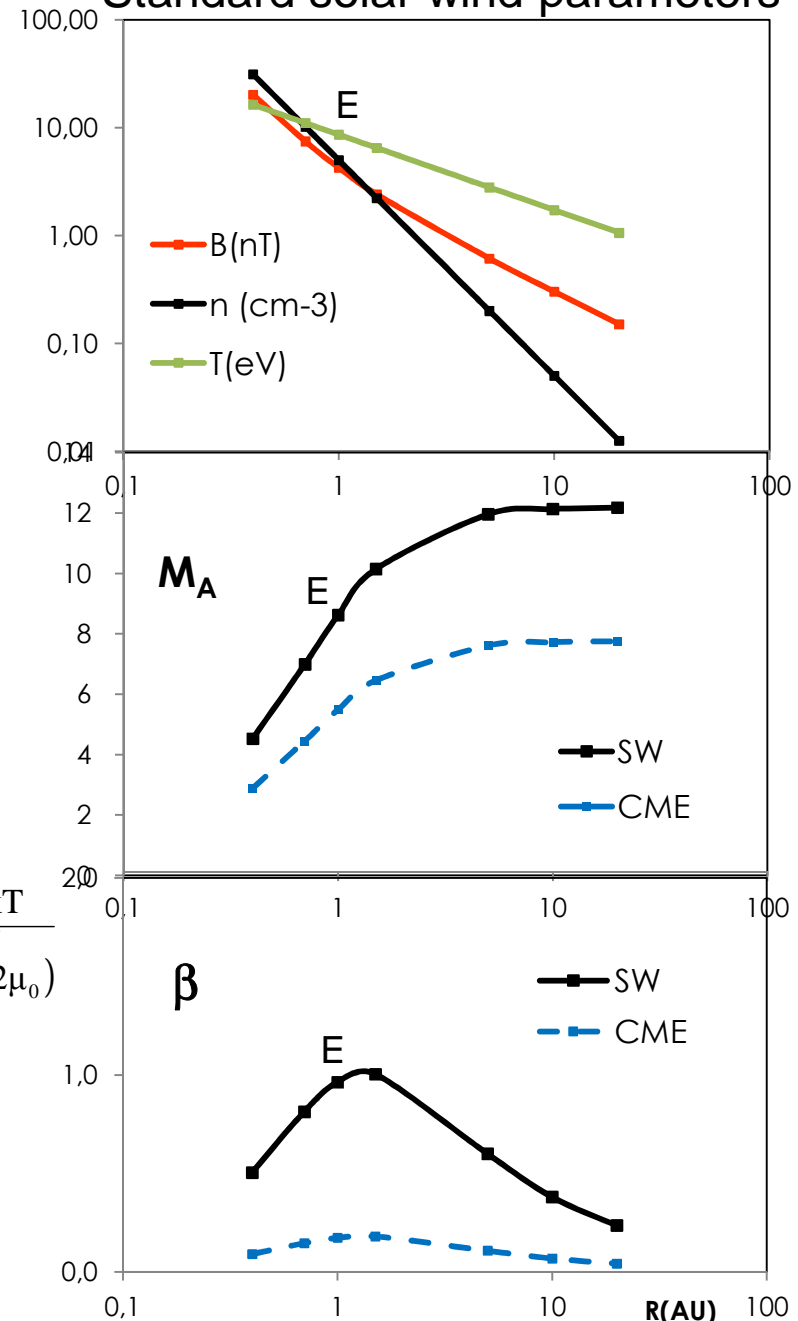


$$M_A = \frac{V}{V_A}$$

$$\beta = \frac{nkT}{B^2 / (2\mu_0)}$$

- Upstream of magnetosphere, formation of a **bow shock** and **magnetosheath region**
- **Important role : magnetosheath plasma** (not solar wind) **interacts with the magnetosphere**

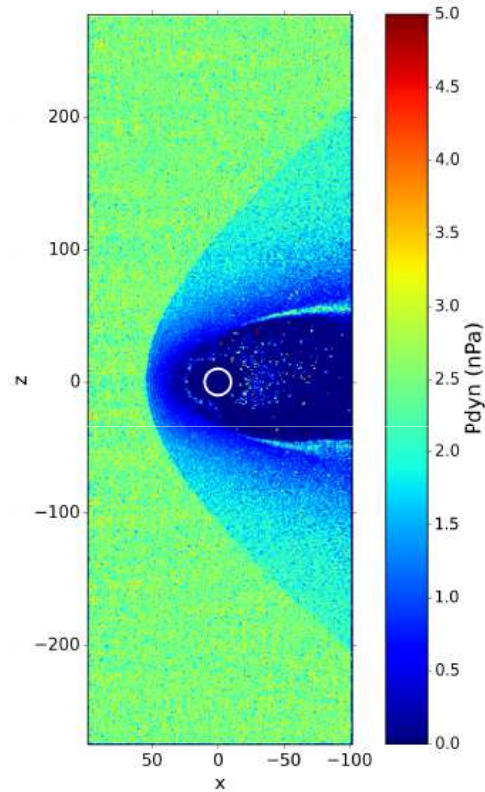
Standard solar wind parameters



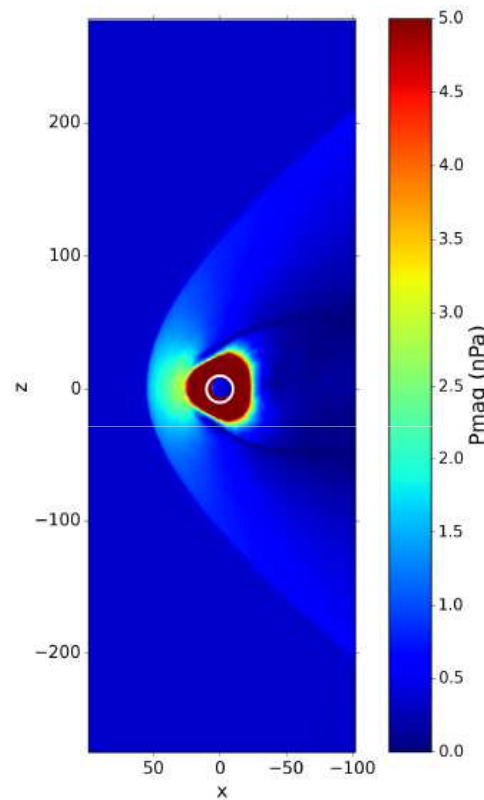
Role of the bow shock :

Conversion of solar wind dynamic pressure into thermal and magnetic pressures

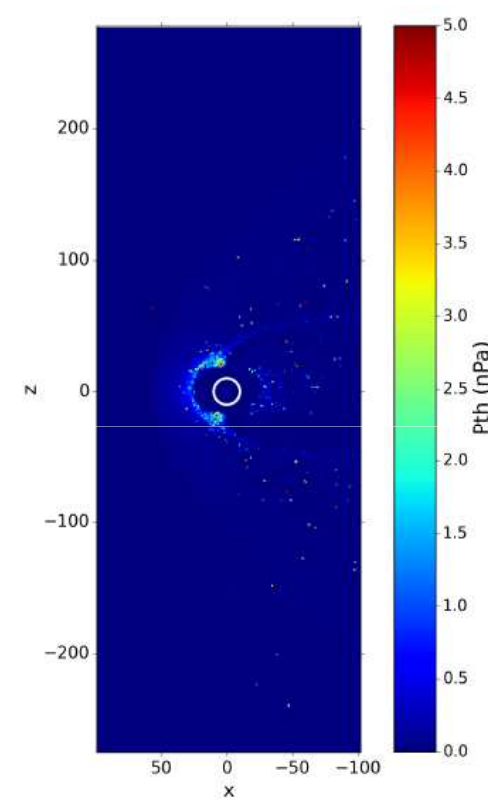
dynamic pressure



magnetic pressure



thermal pressure



Magnetosphere interaction depends on:

- Magnetosheath plasma parameters next to magnetopause : n , \underline{V} , T
- Magnetosheath magnetic field and particularly B_z component (reconnection)
- Magnetosheath electric field : $\underline{E} = -\underline{V} \times \underline{B}$

(Hybrid simulations, L. Turc, thèse, 2014)

Some characteristics of magnetosheath plasma:

Statistical dawn-dusk asymmetries :

(Walsh et al., 2012; Dimmock and Nykyri, 2013) :

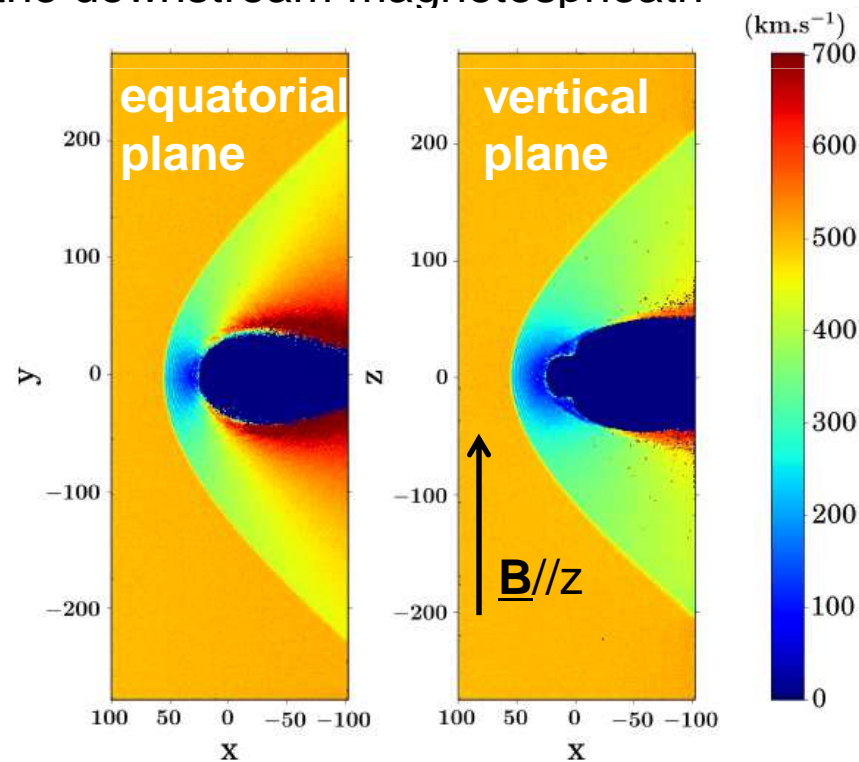
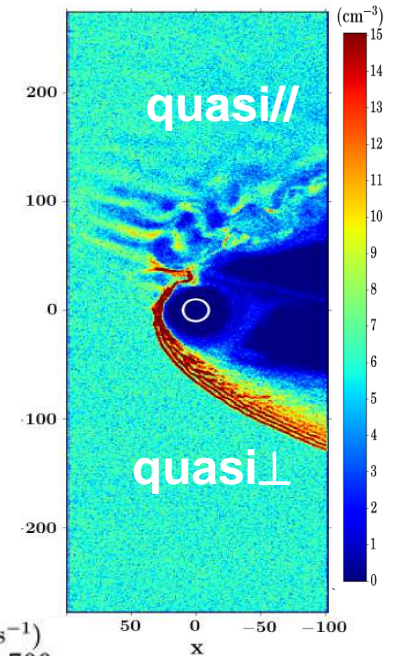
- B dawn $<$ B dusk (max 23%)
- V dawn $<$ V dusk (increasing away from noon) (max 12%)
- n dawn $>$ n dusk (max 21%) but still in discussion

Asymmetrie due to shock configuration: quasi// , quasi \perp :

- fluctuating foreshock region upstream of a quasi // shock
- and also modification of the downstream magnetosphere

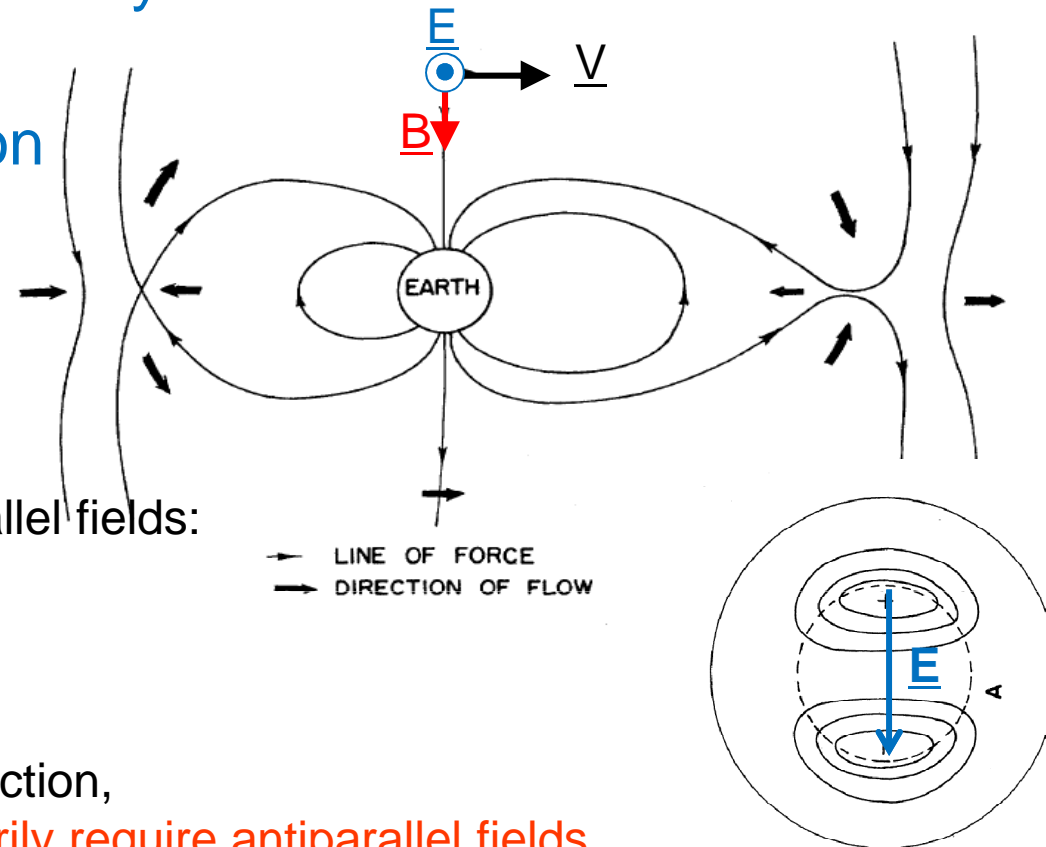
Asymmetries depending on upstream solar wind events:

Ex: CME, magnetic clouds
(low M_A and low β)



Drivers of magnetospheric dynamics

1. Magnetic reconnection



Dungey (1961):

Reconnection between antiparallel fields:
IMF B south and B_{Earth} North

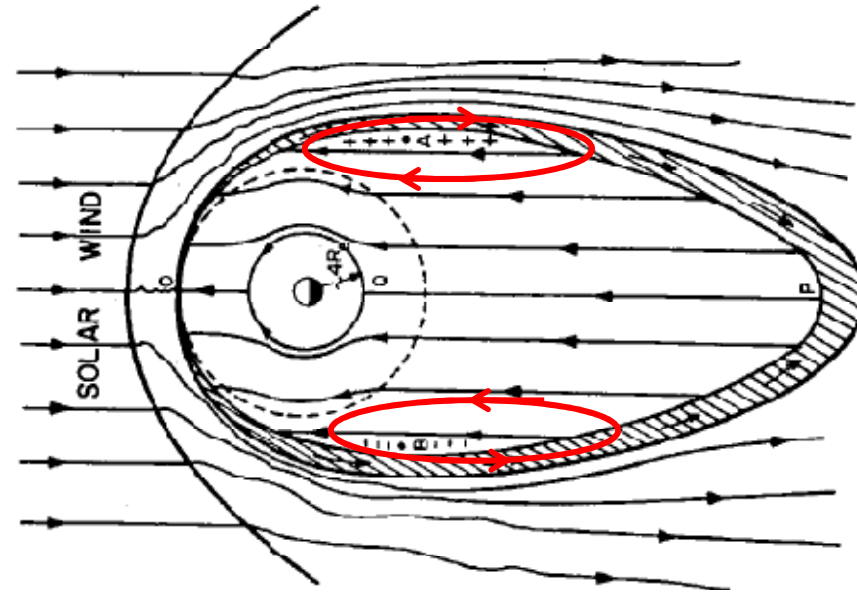
Controlling factors:

- B_{Msheath} components for reconnection,
Reconnection does not necessarily require antiparallel fields
- M_A and β in magnetosheath adjacent to magnetopause
Reconnection **at low magnetic shear** is possible for low β & low M_A in magnetosheath
More precisely : Low $\Delta\beta$ (magnetosheath – magnetosphere)

(Swisdak et al., 2003, Trattner et al., 2007, Trenchi et al., 2008, Phan et al., 2013)

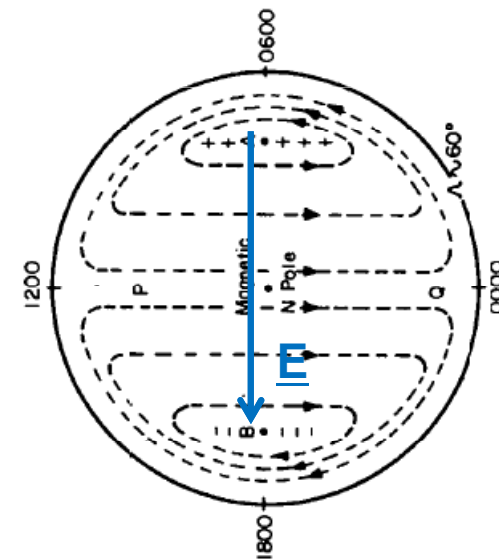
2. Viscous interaction

Proposed by Axford and Hines (1961), Axford(1964)



Viscous drag
→ cross polar cap potential $\sim 20 - 30$ kV

Reiff et al., (1981), Newell et al. (2008)

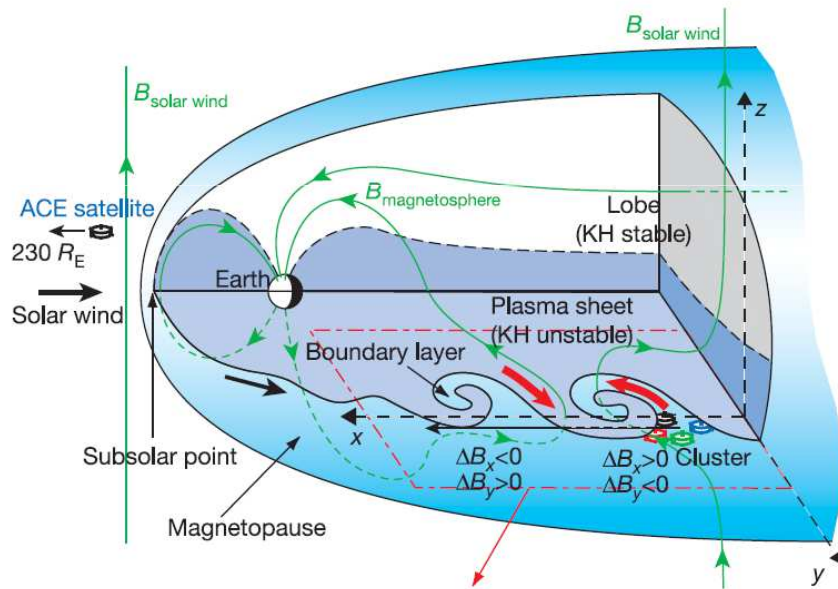


Manifestation of viscous interaction as surface waves and triggering of Kelvin – Helmholtz instability

Triggering condition:
$$\frac{m_0 n_1 n_2}{n_1 + n_2} [\mathbf{k} \cdot \Delta \mathbf{V}]^2 > \frac{1}{\mu_0} [(\mathbf{k} \cdot \mathbf{B}_1)^2 + (\mathbf{k} \cdot \mathbf{B}_2)^2]$$

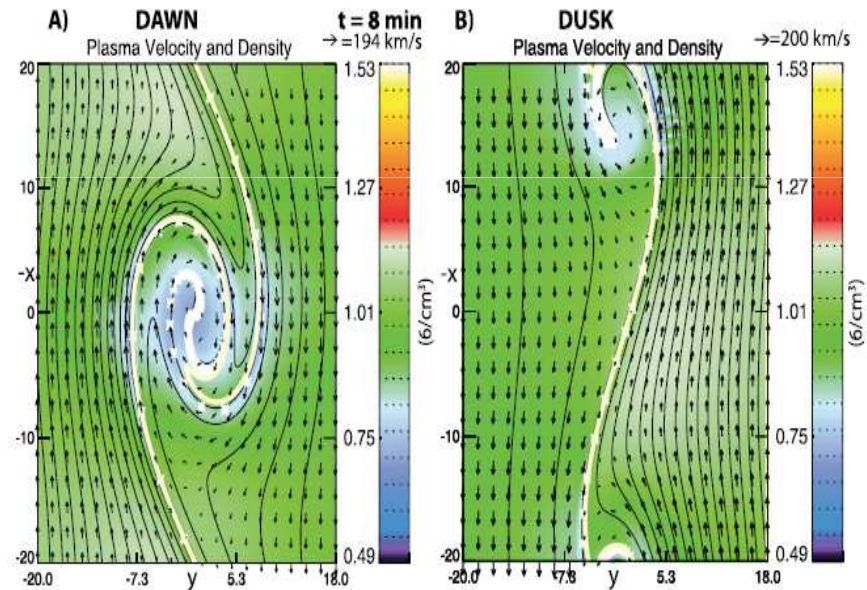
Favorable for:

- Large velocity shears are favorable
- $\mathbf{B} \perp \mathbf{k}$; ($\mathbf{B} // \mathbf{k}$ stabilizes the mode)



Cluster observations
Hasegawa et al., 2004

Many simulations



Dawn-dusk asymmetric development :
growth rates and amplitude larger on
dawnside for Parker spiral

(Nykyri, 2013)

Comments:

- Drivers of magnetospheric activity :

Magnetic reconnection and viscous interaction are responsible

- for matter and energy transfer through magnetopause
- for transport inside magnetosphere

They are not exclusive: both may coexist

- Magnetosheath parameters involved in interaction with magnetosphere:

- **n**: impact on magnetospheric compression

- $\underline{V}_{\text{Msheath}}$: large velocities \rightarrow large shears \rightarrow KH triggering (**viscous interaction**)

- $\underline{B}_{\text{Msheath}}$ in particular B_z component \rightarrow **magnetic reconnection** with B_{planet}
& amplitude $\rightarrow M_A$

- $\underline{E}_{\text{Msheath}} = -\underline{V}_{\text{Msheath}} \times \underline{B}_{\text{Msheath}}$: driver for magnetospheric convection

- **turbulence** \rightarrow implication on heating, temperature and thus on β

Coupling functions between solar wind and magnetosphere:

❖ **Electric field: $E_y = -V B_z$** for southward B_z ; (0 for northward B_z)

Used as proxy for the reconnection rate in antiparallel reconnection

❖ **Akasofu parameter ϵ** (1981): proxy for an energy input rate related to the Poynting

flux : $\underline{E} \times \underline{B} / \mu_0$

$$\epsilon(W) = \frac{4\pi}{\mu_0} V B^2 \sin^4\left(\frac{\theta}{2}\right) l_0^2$$

with : l_0 : an empirical scale factor with a length dimension

θ : clock angle (angle of \underline{B} with Z in the plane transverse to X axis (GSE))

❖ Coupling function based on best correlations between various parameters in solar wind and ground-based indices: (*Newell et al., 2008*)

→ best proxy for **merging rate at magnetopause**: $\frac{d\Phi}{dt} = V^{4/3} B^{2/3} \sin^{8/3}\left(\frac{\theta}{2}\right)$

→ **viscous drag** related to solar dynamic pressure : $n V^2$ or better : $n^{1/2} V^2$

❖ **Rate of flux reconnection** computed by taking into account part of magnetosheath parameters: (*Borovsky, 2013*)

$$R_{2CSB\text{-approx}} = 3.29 \times 10^{-2} \sin^2(\theta/2) n_o^{1/2} v_o^2 M_A^{-0.18} \\ \times \exp\left(-[M_A/3.42]^{1/2}\right)$$

Results :

Table 1. Linear Correlation Coefficients between Various Solar Wind Driver Functions and Various Geomagnetic Indices^a

	$-vB_z$	vB_{south}	Newell	R_1	$R_{2\text{CS}}$	$R_{2\text{CSB}}$	$R_{2\text{CS-approx}}$	$R_{2\text{CSB-approx}}$
AE 1 h lag	0.570	0.687	0.780	0.750	0.774	0.758	0.771	0.766
AU 1 h lag	0.445	0.542	0.650	0.676	0.674	0.665	0.669	0.663
-AL 1 h lag	0.573	0.689	0.764	0.710	0.744	0.727	0.744	0.738
PCI	0.576	0.653	0.757	0.735	0.756	0.744	0.752	0.750
-MBI 1 h lag	0.471	0.605	0.710	0.736	0.730	0.718	0.729	0.723
Kp 1 h lag	0.338	0.535	0.653	0.747	0.704	0.695	0.700	0.696
-Dst* 2 h lag	0.340	0.581	0.634	0.692	0.668	0.668	0.660	0.667
7-Index Sum	3.313	4.292	4.948	5.046	5.050	4.977	5.025	5.003

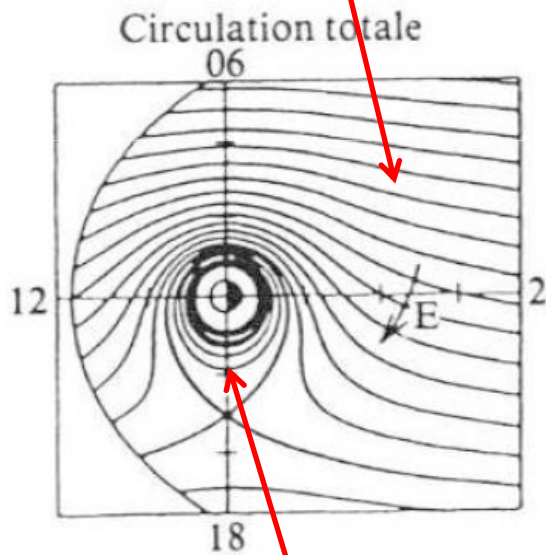


Borovsky (2013)

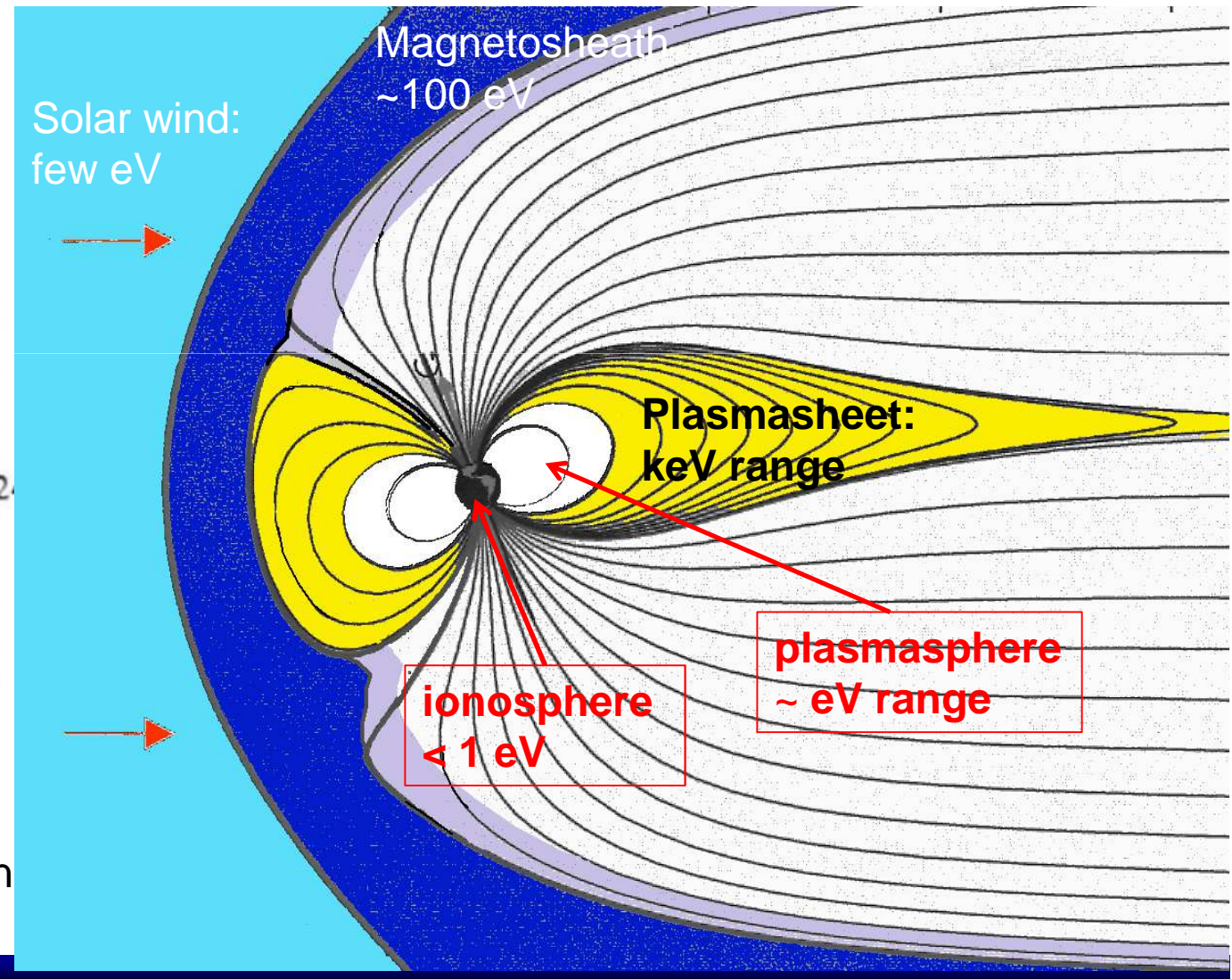
Far from a 100% reliable description of the solar wind / magnetosphere coupling !

2. Dynamics of the coupled magnetosphere - ionosphere system

Plasmasheet:
dominated by
convection

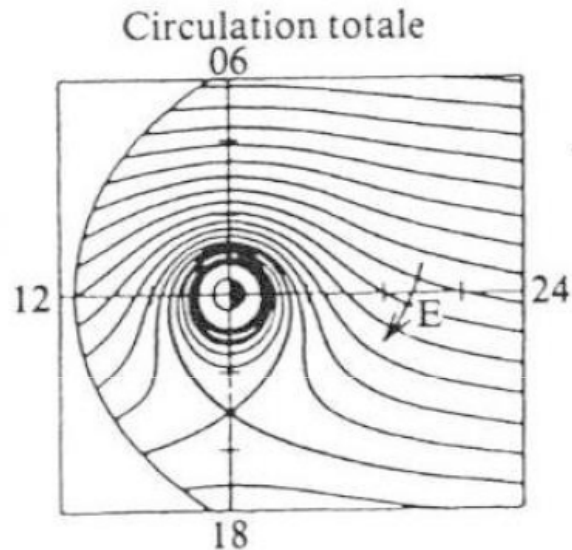


Plasmasphere:
dominated by corotation

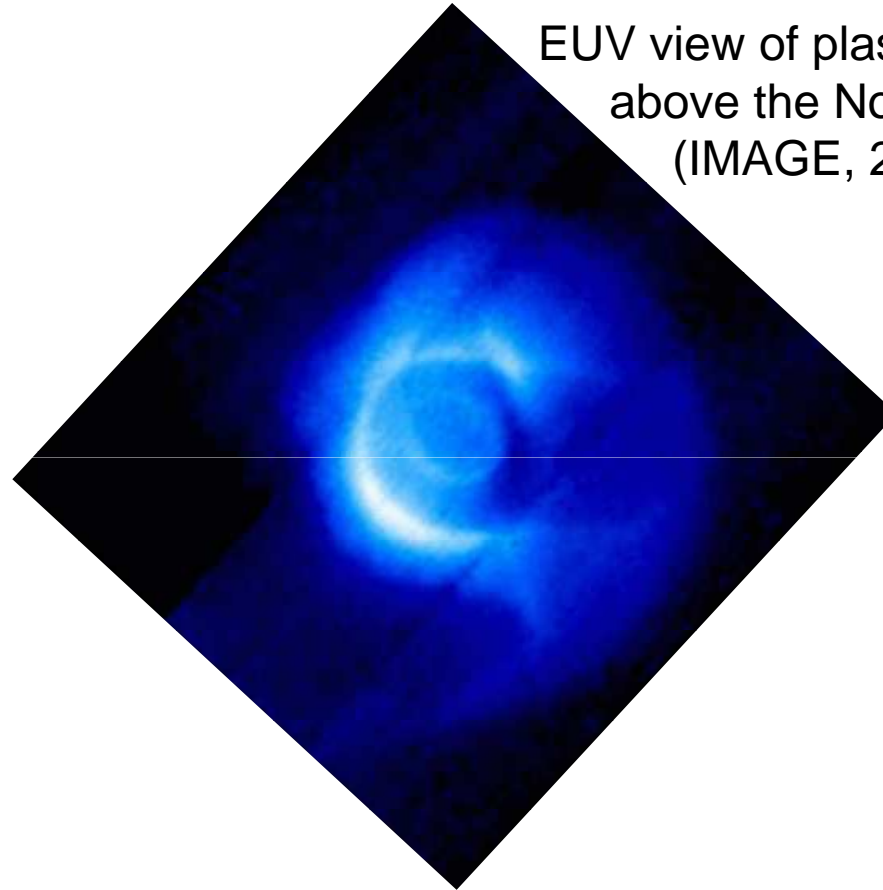


Plasmasphere:

Cold plasma of ionospheric origin, ~ co-rotating with the planet



EUV view of plasmasphere
above the North pole
(IMAGE, 2000)



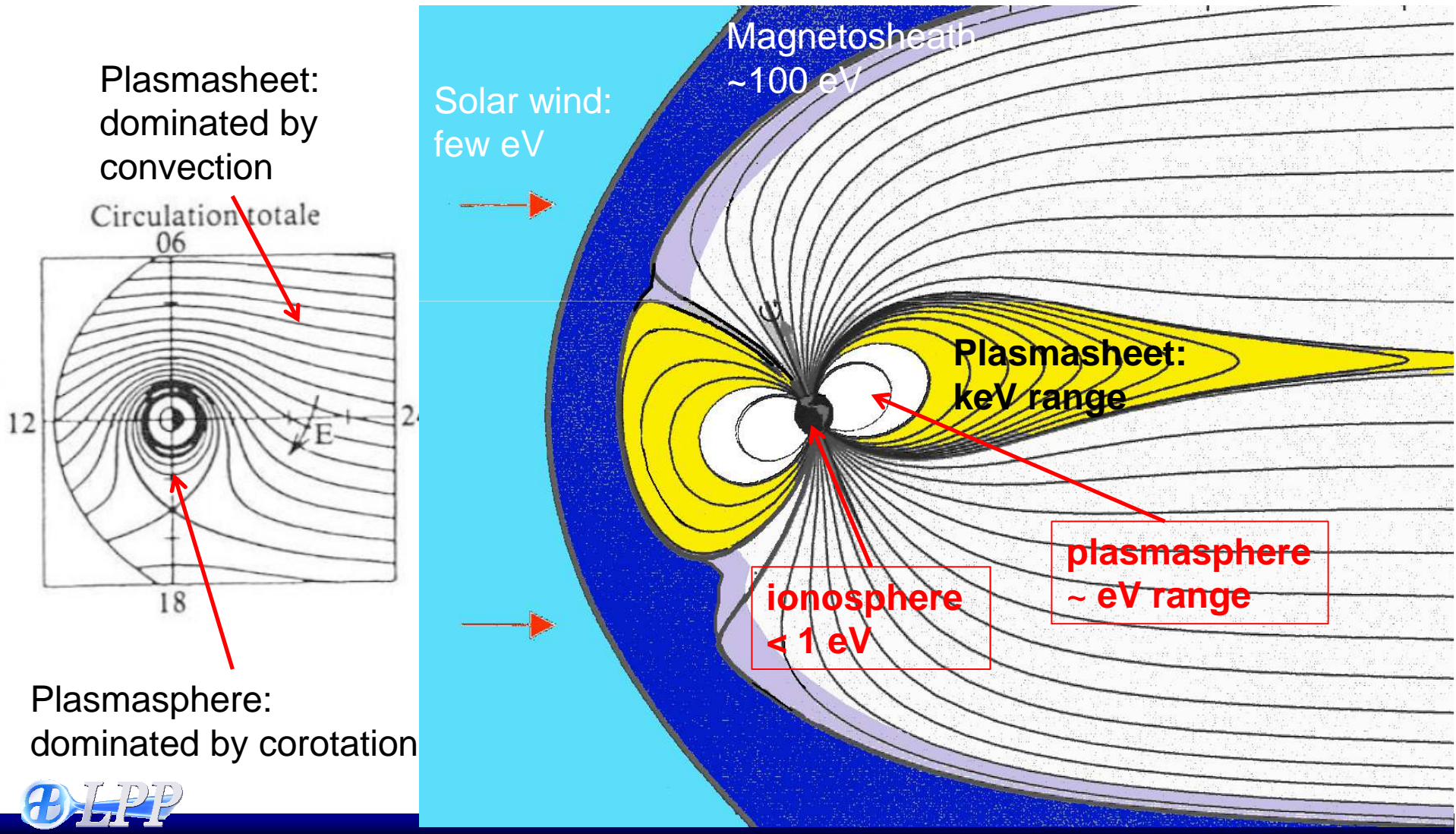
Transport of cold plasma outwards towards the dayside :

- **plumes** related to convection variations during active periods
- or « **plasmaspheric wind** » flowing even during quiet periods

(Dandouras, 2013)

Plasmasheet: essential region for magnetospheric activity

- convection regime from nightside to dayside
- strong ionosphere – magnetosphere coupling on closed field lines
- substorms development and auroral activity (see talk by Olivier)



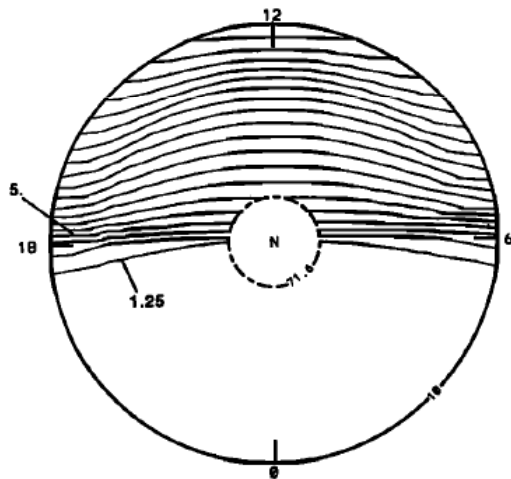
Ionospheric dynamics (on closed magnetic field lines connected to plasmasheet)

Transport in the ionosphere described by the ionospheric electric field: $\vec{E}_I = -\vec{\nabla}\Phi$
 with Φ , convection electrostatic potential is solution of the current closure equation in the ionosphere:

with Ohm's law: $\vec{j}_I = \sigma \cdot \vec{E}$ and σ ionospheric conductivities

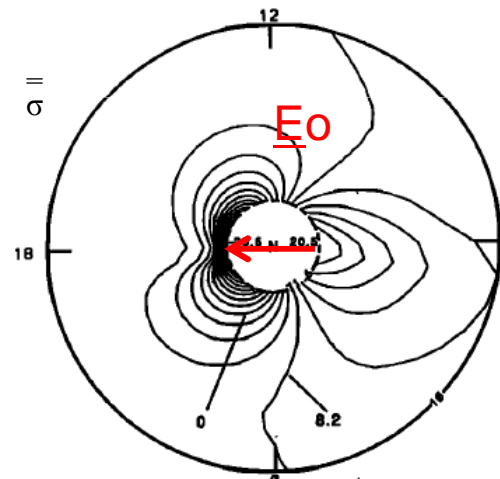
At initial state, ionospheric conductivities are only due to solar illumination:

PEDERSEN CONDUCTIVITIES, INITIAL STATE



24
conductivities

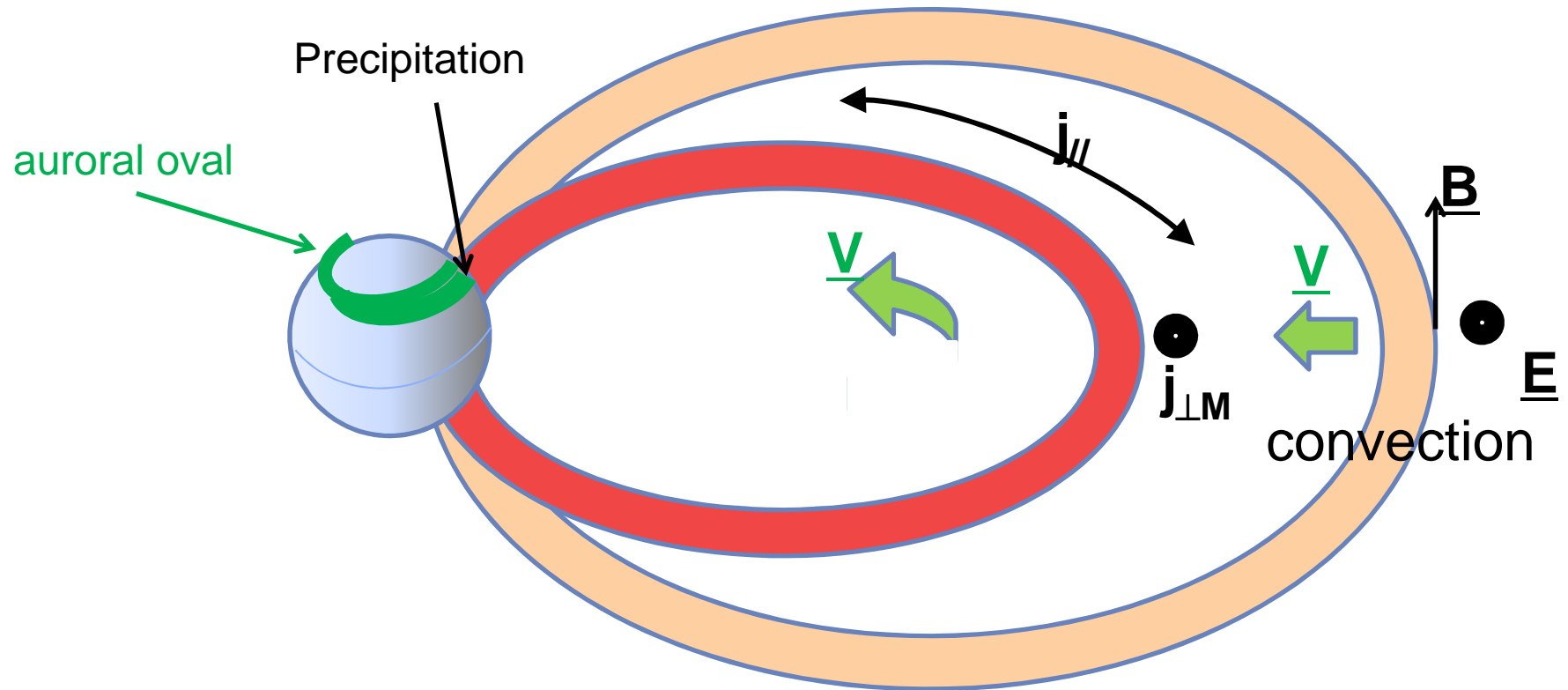
CONVECTION POTENTIAL, INITIAL STATE



convection electrostatic potential Φ

→ Transmission of Φ along closed magnetic field lines to the magnetic field lines

Coupled Plasmasheet – Ionosphere transport (closed field lines)



→ Need for a self-consistent description of the coupled transport in the ionosphere and magnetosphere

Description:

Magnetospheric transport : ex: multi-fluid equations

$$\rho_j m_j \frac{d\vec{V}_j}{dt} = \rho_j q_j (\vec{E} + \vec{V}_j \times \vec{B}) - \vec{\nabla} P_j \quad \begin{array}{l} + \text{ density equation} \\ + \text{ energy equation} \end{array}$$

$\rightarrow \underline{\mathbf{J}}_{\perp M}$

Ionospheric Ohm's law: $\vec{J}_{\perp I} = \overline{\Sigma} \cdot \vec{E}_I$

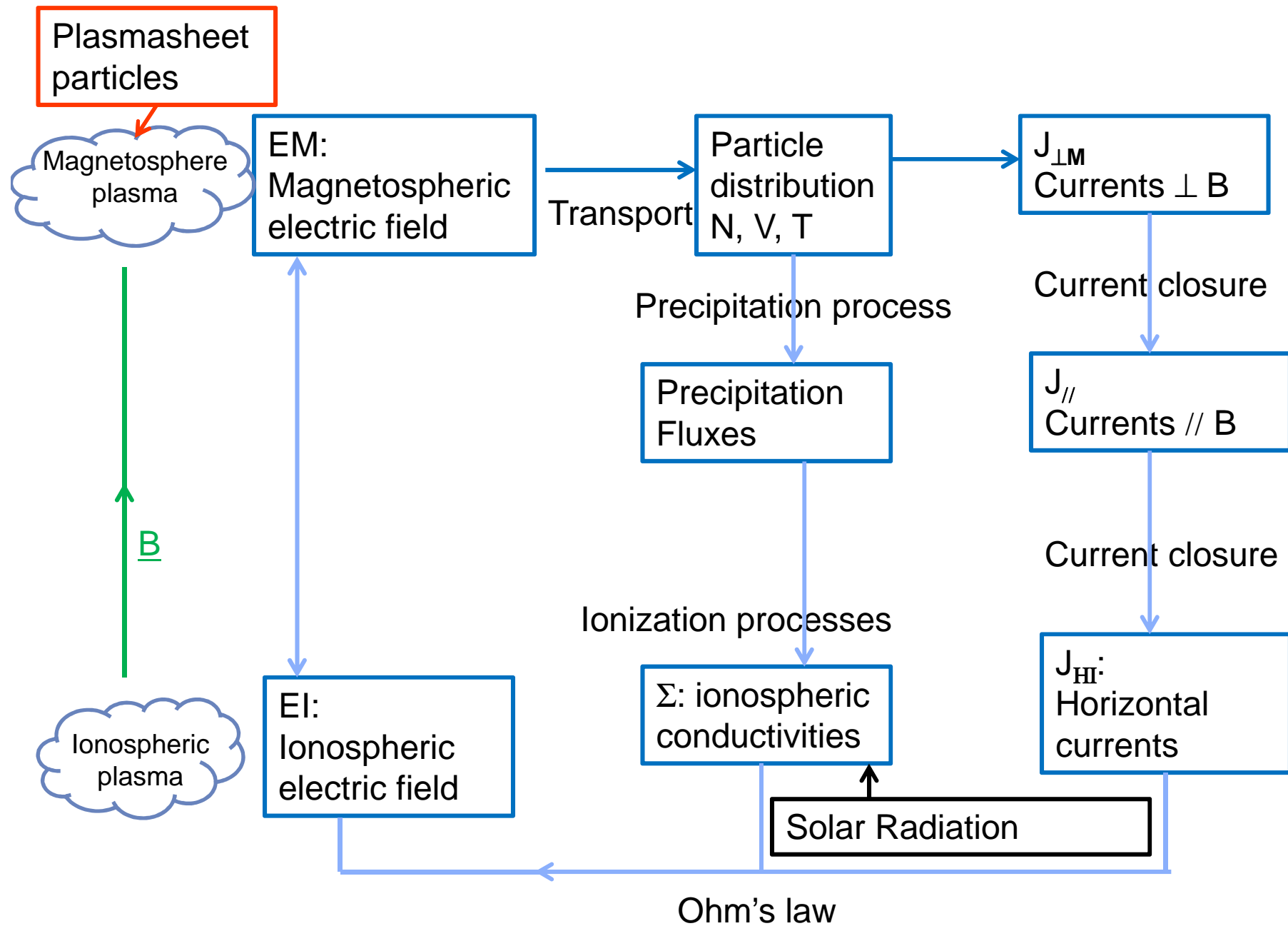
Magnetosphere / ionosphere couplings along magnetic field lines:

- Transmission of electric field
- Precipitation in ionosphere of magnetospheric particles
→ enhancement of ionospheric conductivities
- Current closure : $\text{div} (\mathbf{J}_{\perp} + \mathbf{J}_{\parallel}) = 0 \rightarrow \mathbf{J}_{\parallel}$

Simulations:

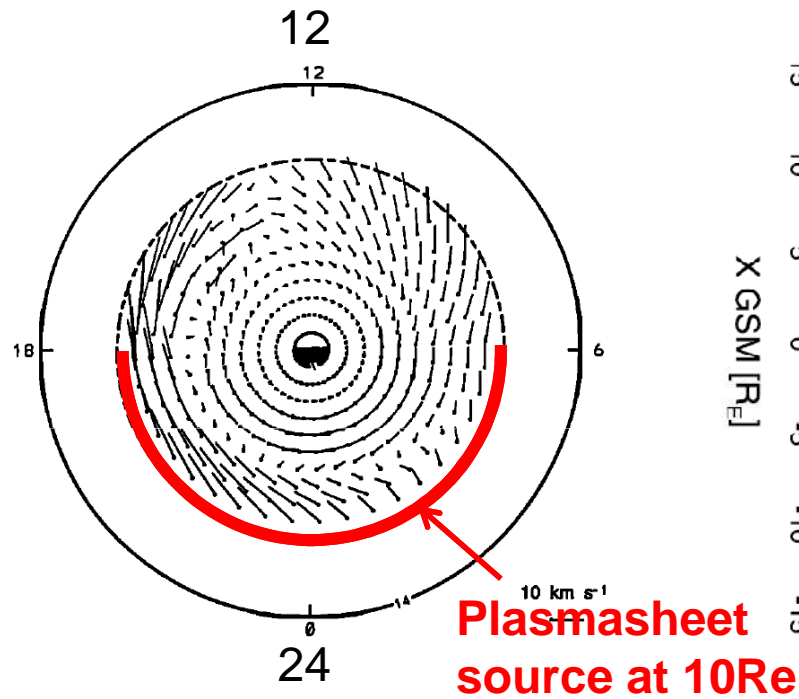
- Different models focuses on magnetosphere or ionospheric transport
- A few with self-consistent approach of the coupling:

(Fontaine et al. 1985; Peymirat et al. 1994 / Harel et al. 1981; Wolf et al., 2007)..)

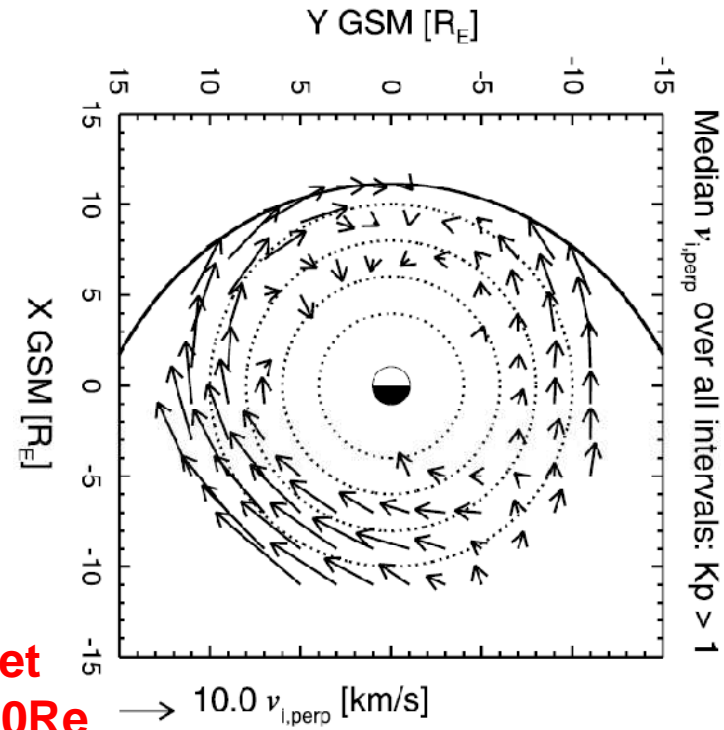


Magnetospheric transport

Ion Velocity



Simulations
(Peymirat & Fontaine, 1994)

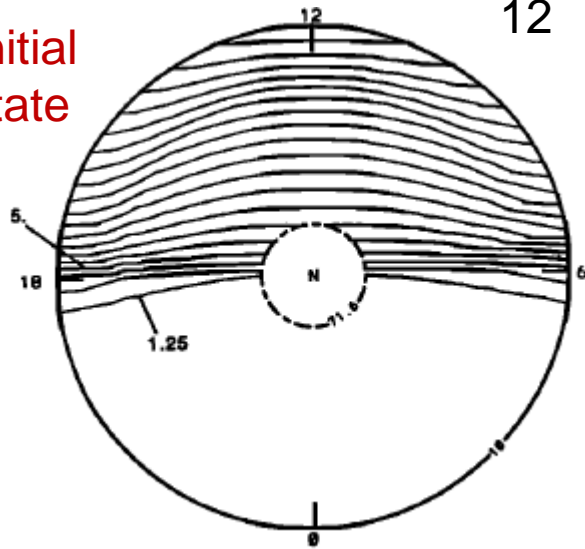


THEMIS statistics
(Lee & Angelopoulos, 2014)

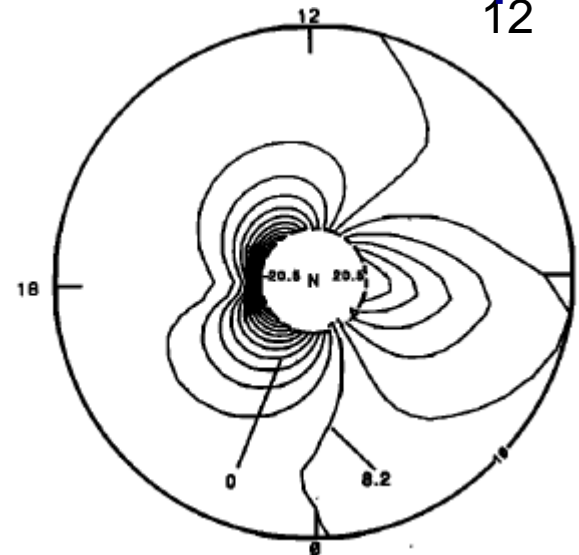
IONOSPHERE: $\sim 0^\circ \rightarrow 90^\circ$ latitude

Pedersen Conductivities

Initial state

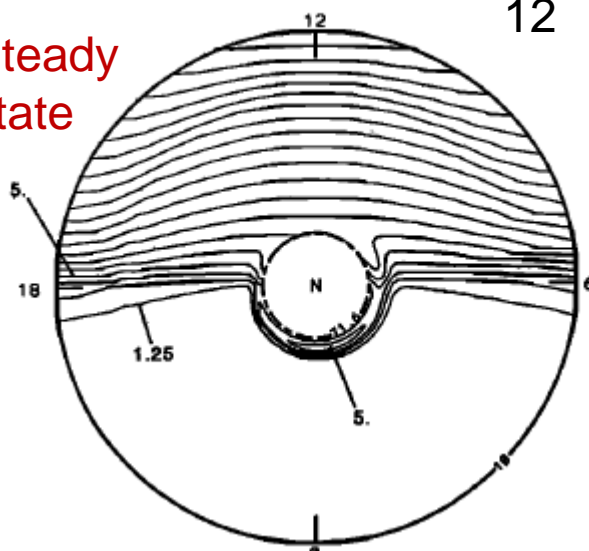


Electrostatic iso-potentials

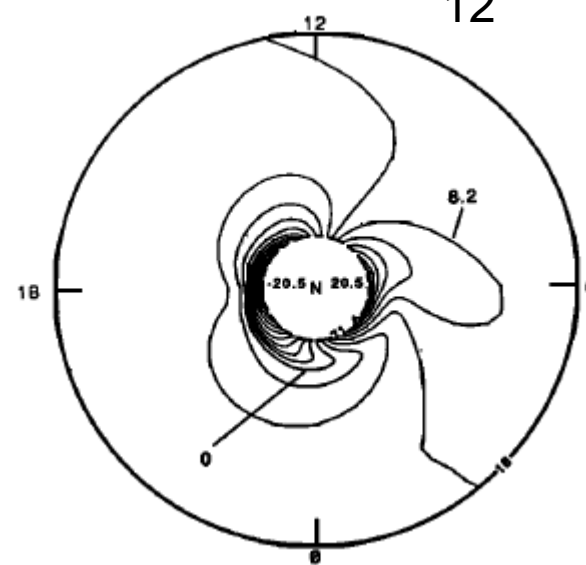


PEDERSEN CONDUCTIVITIES, STATIONARY STATE

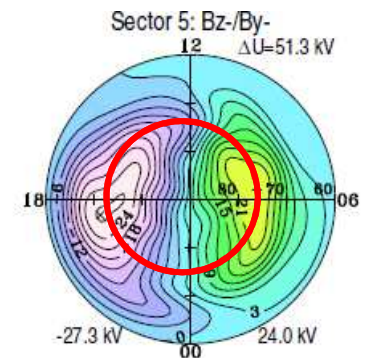
Steady state



CONVECTION POTENTIAL, STATIONARY STATE



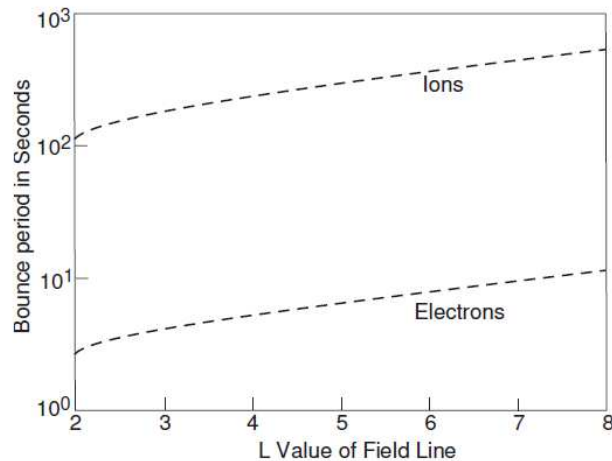
Cluster (EDI) observations
(Haaland et al., 2007)



For events occurring on time scales < bounce periods

few minutes for keV ions

few seconds for keV electrons



For 1keV-particles
at 30° pitch-angle

→ particles may,be not available to carry required currents between ionosphere and magnetosphere and close the planetary circuit

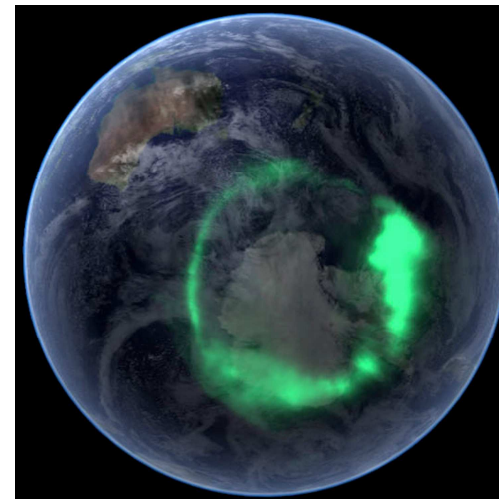
→ acceleration processes of ionospheric or magnetospheric particles
injection of energetic particles into inner regions
wave-particle interaction processes
(see presentations by Nicole and Patrick)

Ex: Case of substorms:

Sudden magnetic reconfiguration
(see presentation by Olivier)

Localized particle accelerations
produce discrete arcs

Injection of particles towards ring current
and radiation belts



3. Particle sources and outflows

In the absence of active moons, only 2 sources available in the terrestrial environment:

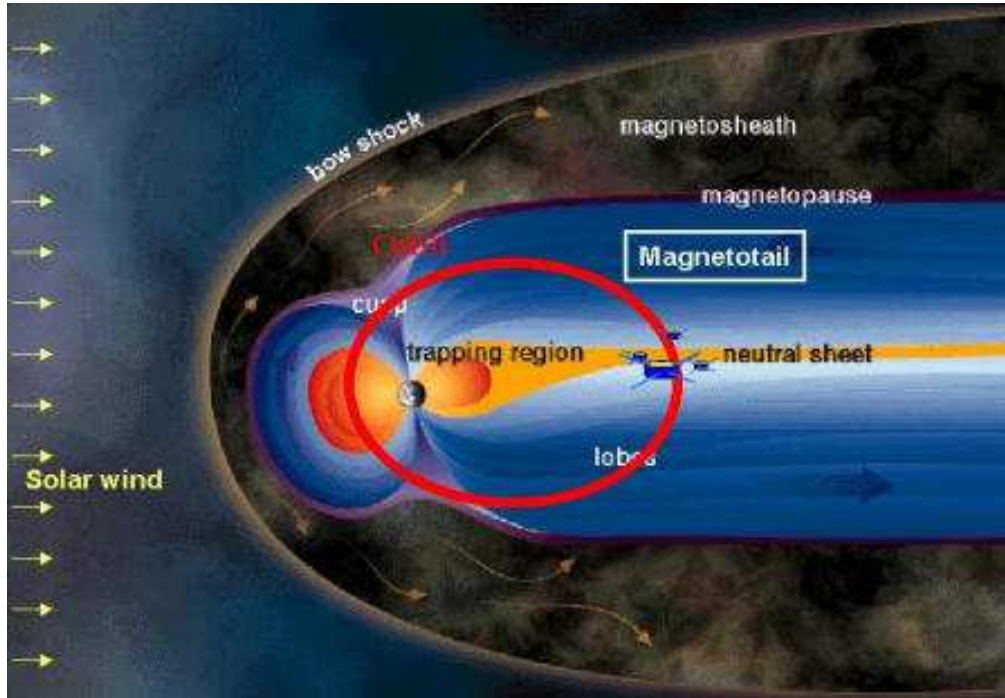
❖ **Solar wind:**

- Reconnection processes between planetary and interplanetary magnetic fields
 - Entry through via cusp regions or high-latitude magnetopause
 - Anti-sunward convection above polar cap
 - + dayside return with energy gain: hot plasmasheet
- Viscous interaction (Kelvin Helmholtz at low latitude):
 - Entry through low-latitude flanks of magnetopause: cold dense plasmasheet

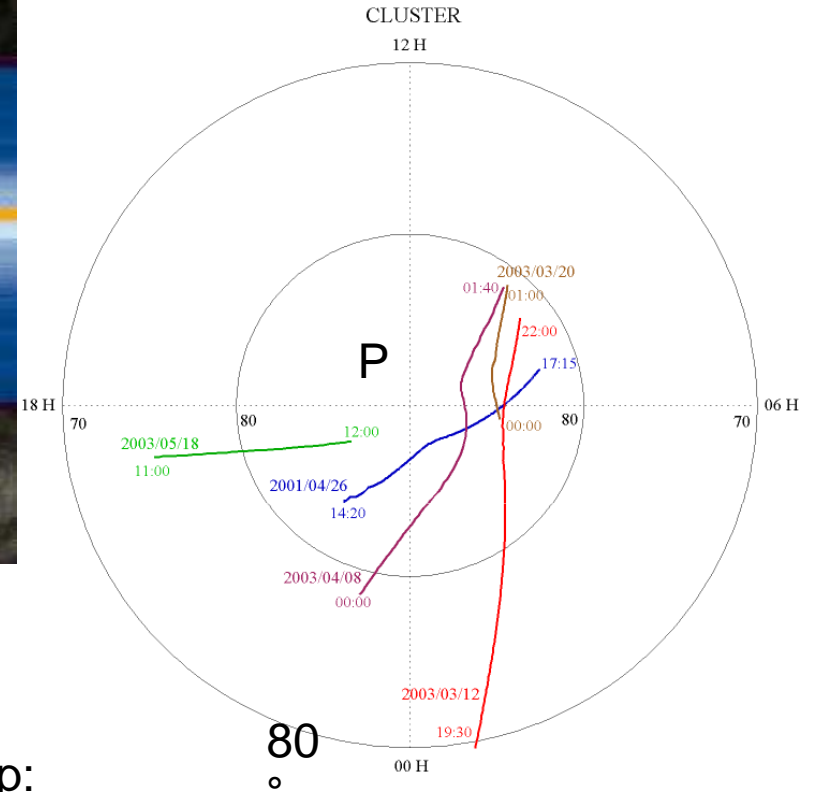
❖ **Ionosphere**

- Various types of outflowing ions:
 - Polar wind and polar cap outflows
 - Ion upwelling from polar cusp/cleft ion fountain,
 - Upward ion conics and beams from auroral zone
- Various acceleration processes
 - Parallel electric fields
 - Transverse ion acceleration
 - Wave particle instabilities

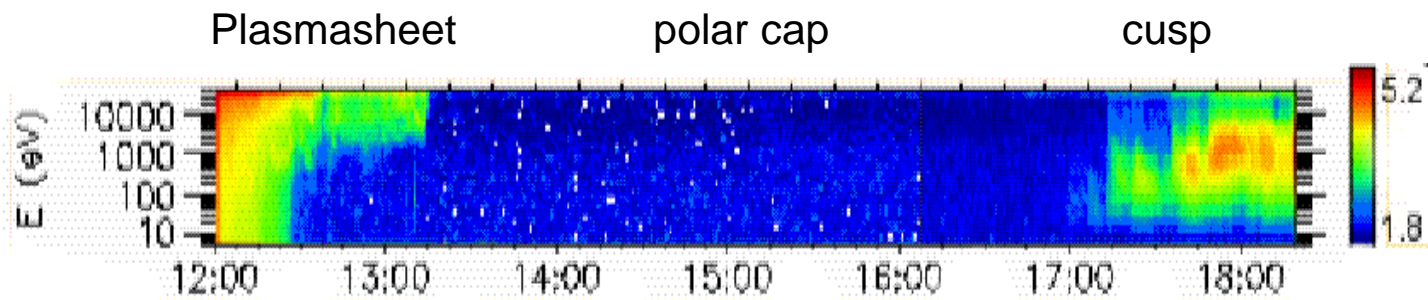
(see reviews by Yau and André, 1997; André and Yau, 1997, Moore et al, 1999)



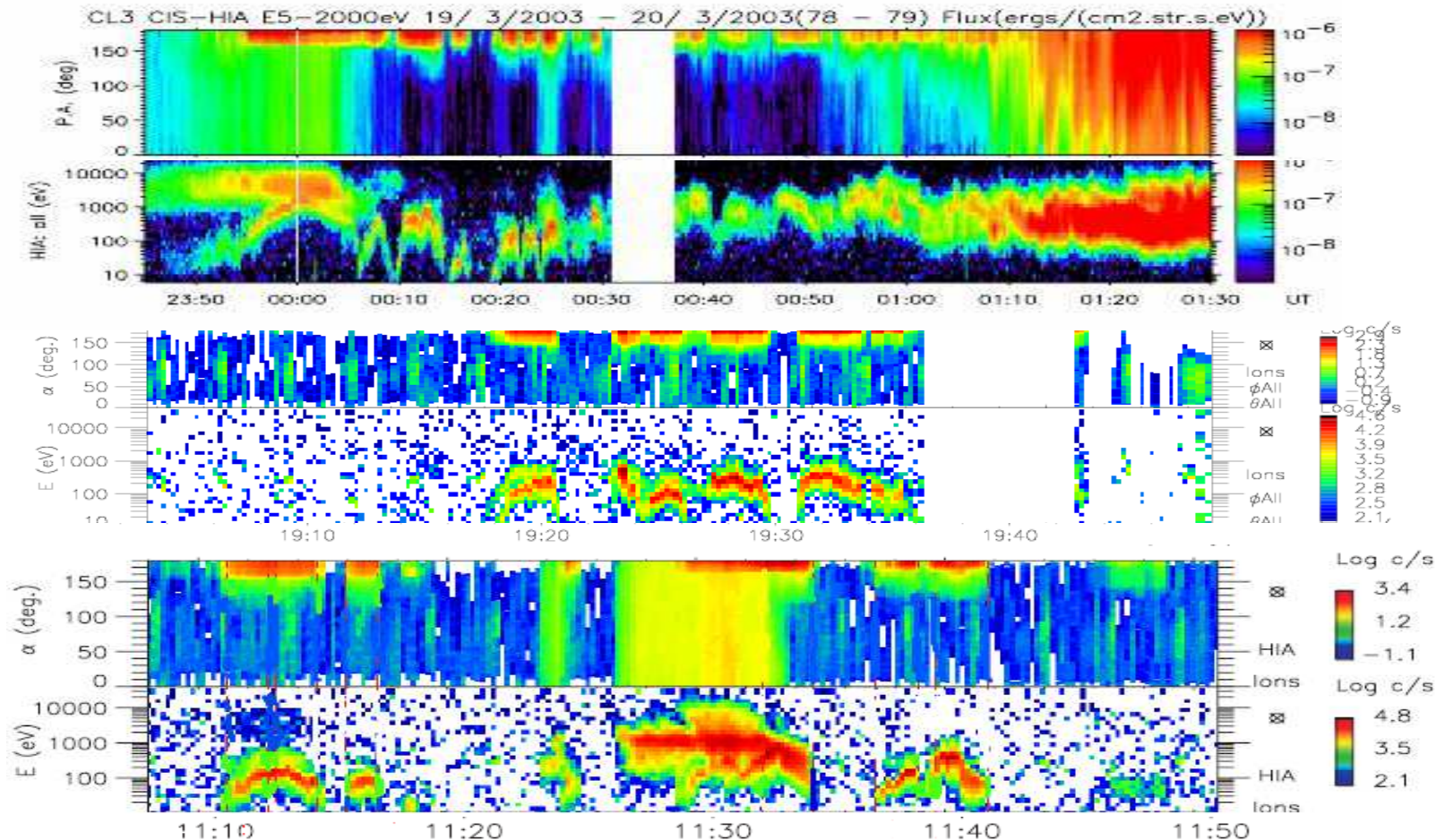
CLUSTER polar cap orbits



Standard CLUSTER observations above polar cap:



Ion outflows during quiet periods, weak or northward IMF:



At quiet time, successive structures of ion outflowing beams along CLUSTER orbit.
 Typical inverted V shape → acceleration by field-aligned potentials above polar cap
 (Maggiolo et al., 2006; Fontaine et al., 2006, Teste et al., 2007; Maggiolo et al., 2011)

Question: In the absence of acceleration, are there also ion outflows at lower energy ?
 Indeed, positively-charged satellite cannot detect low-energy ions

Statistics on cold ions:

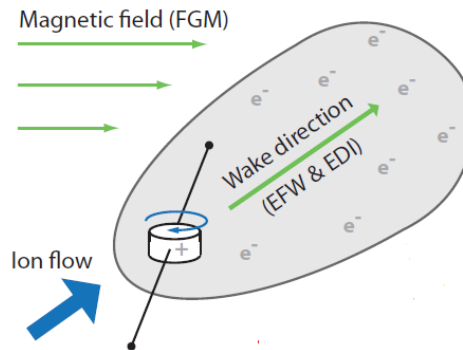
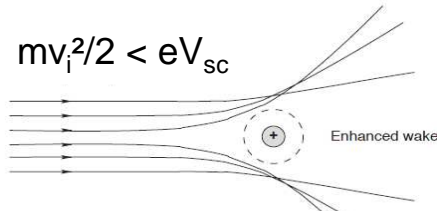
Measurement of positive ion flows onboard a positively-charged satellite (Cluster):

For ion beams with $mv_i^2/2 > kT_i$, if $mv_i^2/2 < eV_{sc}$, ions cannot be detected by ion sensors

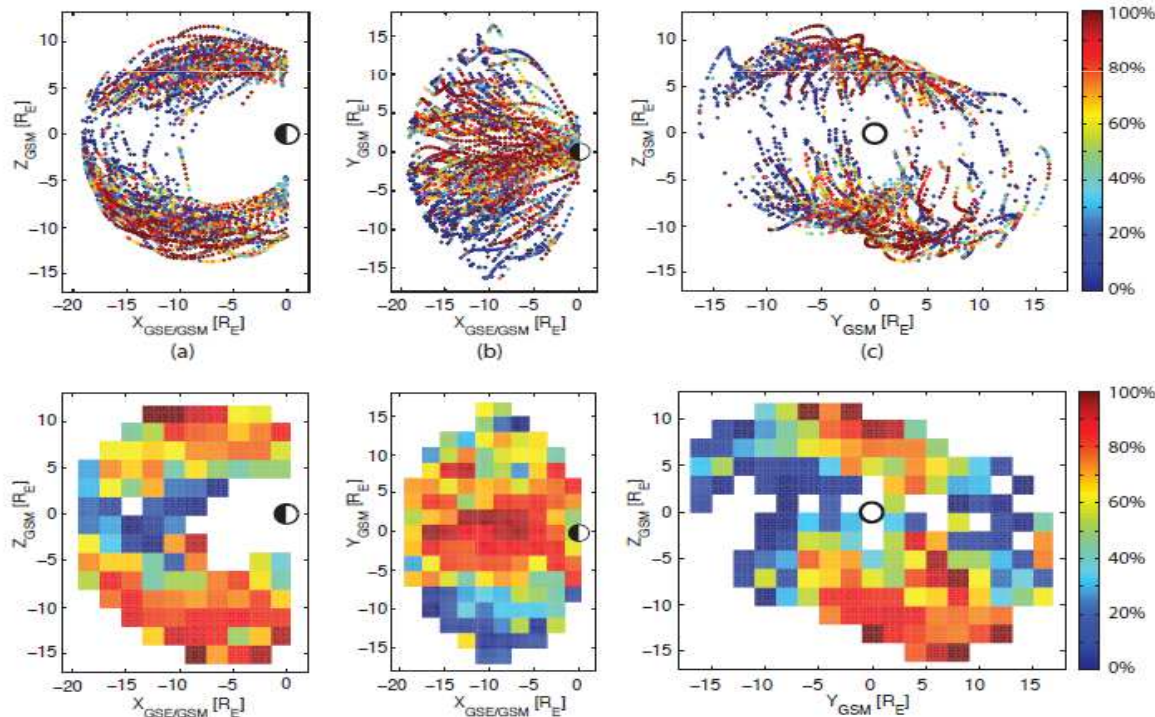
$$mv_i^2/2 \gg eV_{sc}$$



$$mv_i^2/2 < eV_{sc}$$



With long boom antennas, electric field measurements (EFW) detects the flow direction & amplitude and density of cold ions



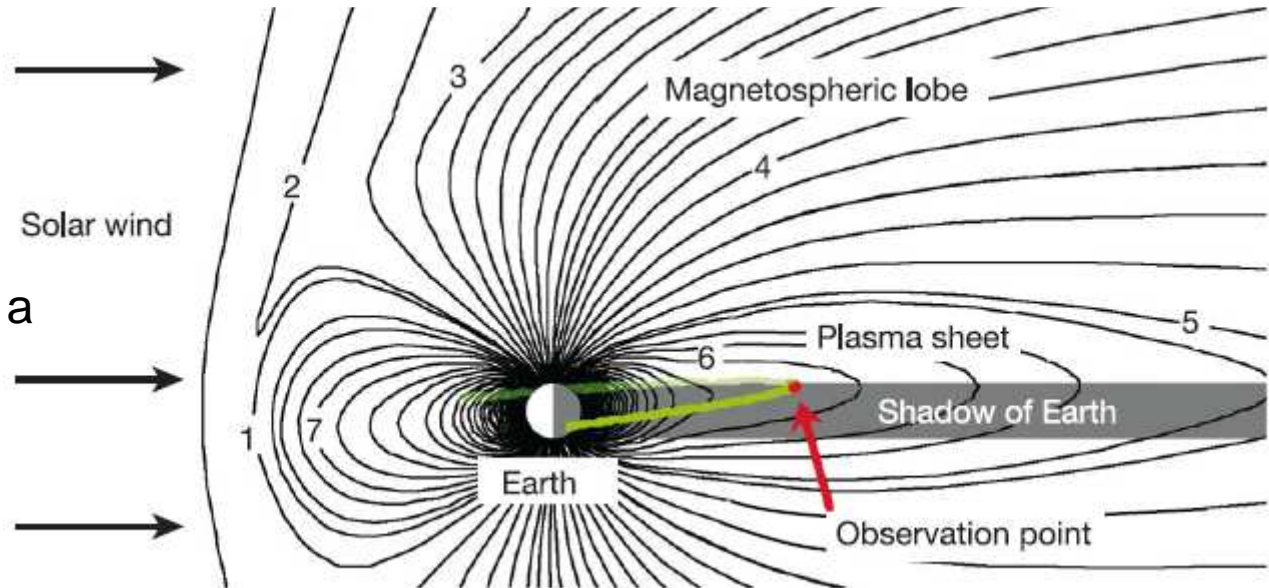
Cold ions escaping from ionosphere dominate both in flux and density large regions of magnetosphere

Lobes & polar regions are found full of cold plasma not detected by ion sensors.

(Engwall et al., 2009; André and Cully, 2012)

Plasmasheet

Geotail observation during a solar eclipse
(Seki et al. 2003)

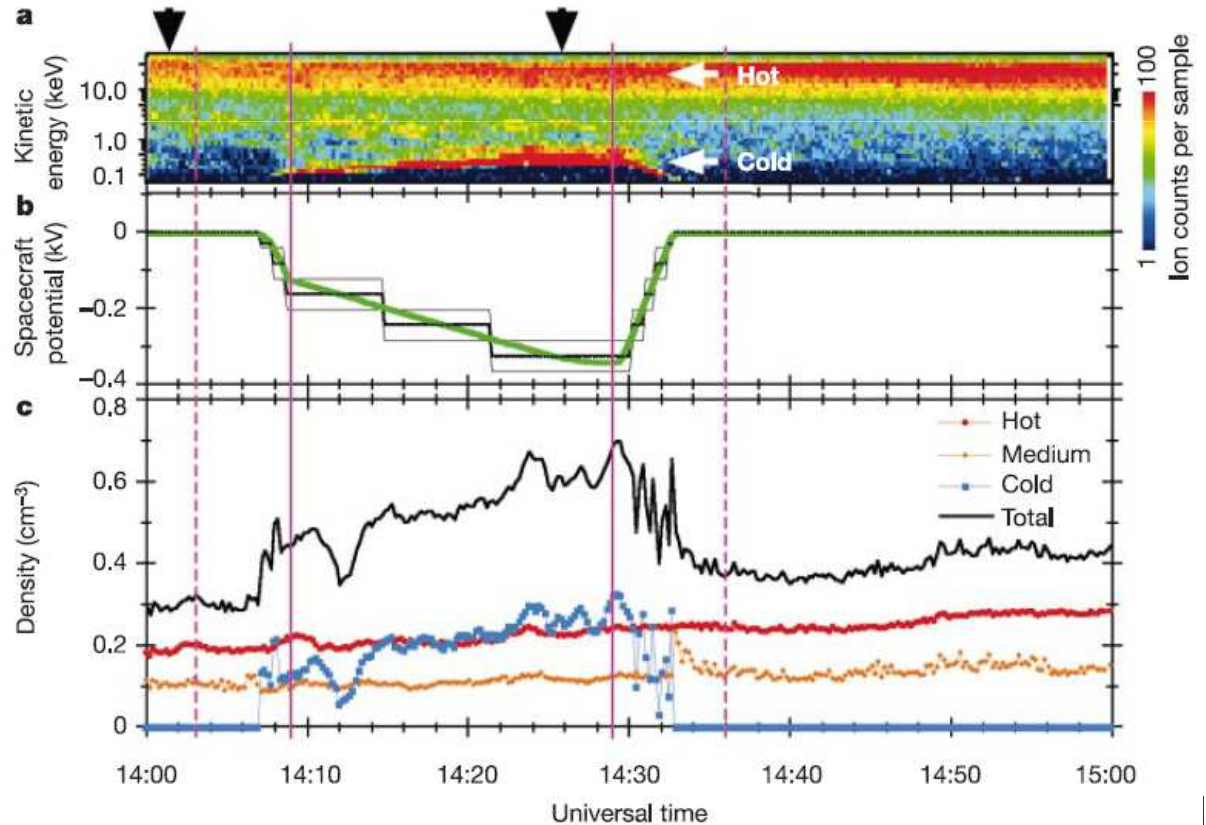


Appearance of a very cold ion population,

- accelerated by a negatively-charged spacecraft

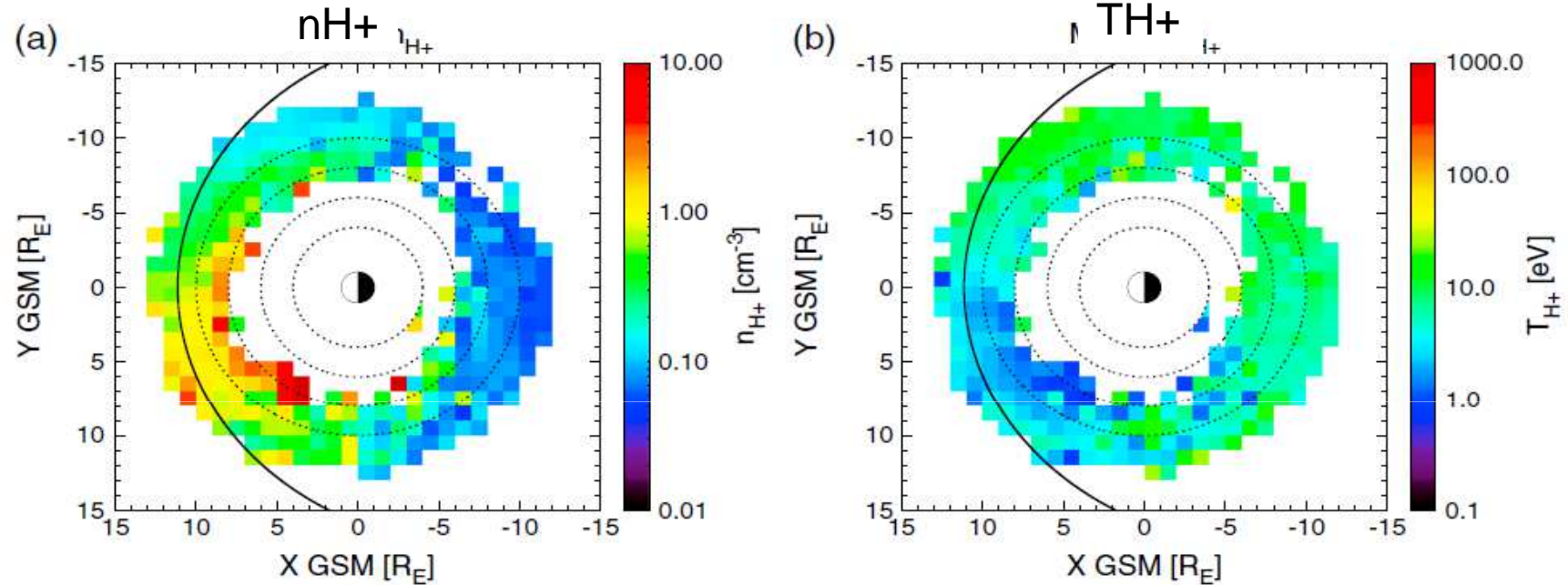
- comparable or larger density than hot plasmasheet population

This population is too cold to be detected by particle sensors outside eclipses: Ionospheric origin ?



Themis statistics on cold ions in equatorial plane ($< 10 R_E$)

(Lee & Angelopoulos, 2014)



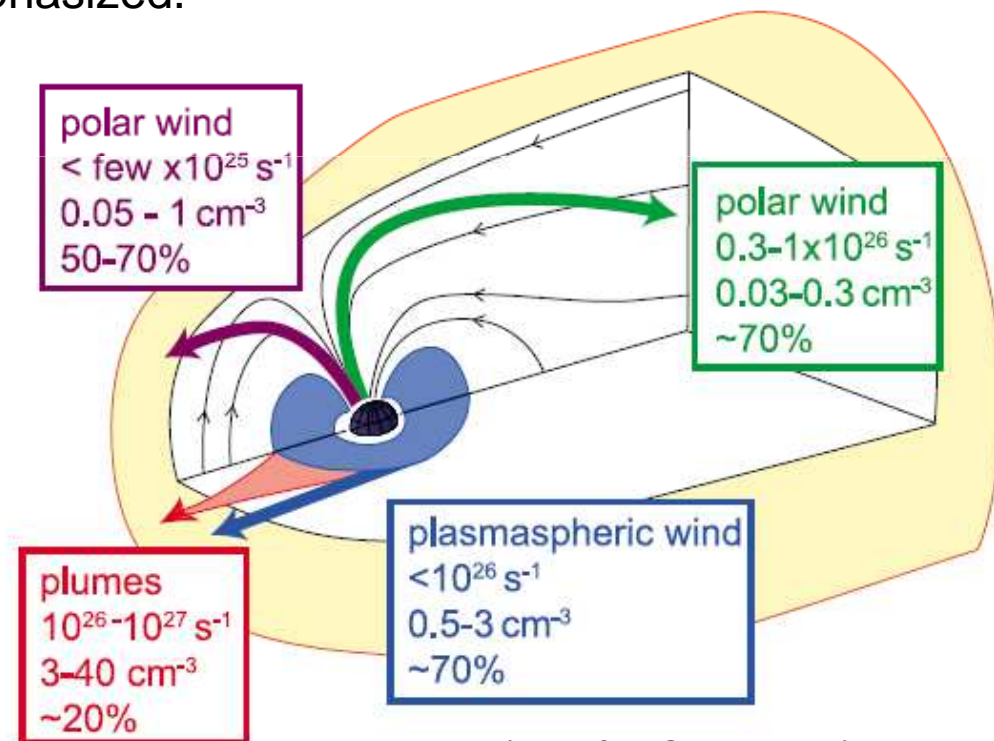
- High densities of cold protons (~ 1 eV) in post noon sector
- Implications on dayside physics (loss of plasma on dayside, role on dayside reconnection process)

Finally, **ion sensors cannot detect cold ionospheric ions** unless they are accelerated or during particular events (eclipses).

Statistics from indirect methods show that large fluxes of low-energy ions escape from the ionosphere and dominate the density of most magnetospheric regions and most of the time.

They represent a more important plasma source or for the terrestrial magnetosphere that previously emphasized.

A significant fraction can also be lost on the dayside or at polar latitudes.



(André & Cully, 2012)